

## **Multimaterial Aerosol Jet Printing of Passive Circuit Elements**

S. J. Johannes<sup>1</sup>, D. M. Keicher<sup>2</sup>, J. M. Lavin<sup>1</sup>, E. B. Secor<sup>1</sup>, S. R. Whetten<sup>1</sup>, M. Essien<sup>2</sup>,

<sup>1</sup>Sandia National Laboratories, P.O. Box 5800, Albuquerque, NM 87185

<sup>2</sup>Integrated Deposition Solutions, Inc.

### **Abstract**

Recent advances in additive manufacturing technologies present opportunities for rethinking the design and fabrication of electronic components. An area of considerable interest for electronic printing is the production of multi-layered, multi-material passive components. This research focuses on the design and fabrication of a toroidal microinductor using a digital, direct-write printing platform. The toroidal inductor has a three layer design with a dielectric and core material printed in between the lower and upper halves of the conductive coil. The results of this work are discussed, including printer, ink, and processing requirements to successfully print the multi-layer, multi-material component. The inductance of several successful printed devices is measured and compared to predicted values. Overall, the results and lessons of this work provide guidance for future work in this growing field.

### **Introduction**

Printed electronics technology has many advantages over traditional electronics manufacturing, including compatibility with flexible form factors, high throughput and large-area fabrication, and broad materials compatibility [1]. In addition, these technologies can be easily embedded in additive manufacturing process flows, with digital control enabling rapid prototyping and custom fabrication. Aerosol jet printing techniques, in particular, offer a promising digital, non-contact, direct-write solution for device prototyping. The NanoJet printer, developed by Integrated Deposition Solutions, Inc., can print a wide range of nanoscale materials with high resolution, and supports straightforward interchangeability of inks for integrating multiple materials. [2] As these technologies advance, more sophisticated multi-layer, multi-material integration becomes possible, offering opportunities for printing passive electronic components [3-5]. Among electronic circuit components, passive elements such as capacitors and inductors are critical for complex circuit designs, and require integration of multiple materials. Inductors are widely used in applications such as signal filtering, and often require a large volume, motivating the development of additive fabrication routes for miniaturized designs [6]. A basic inductor contains a coil of wire wrapped around a magnetic or dielectric core, which stores energy by resisting the change in current through the coil. This stored energy is related to the inductance of the device, measured in units of henrys. For a conventional inductor geometry, the inductance is directly proportional to the number of turns in the coil, cross sectional area of the core, and permeability of the core, and is inversely proportional to the circumference around the inductor.

Inductors commonly have toroidal or solenoidal geometries, containing disk-like and solid cylindrical cores, respectively. Both have wire wrapped around them to create a magnetic

field. Magnetic leaking at the ends of solenoidal designs reduces the inductance and can lead to interference with other circuit elements, motivating the selection of a toroidal inductor for this research.

The permeability and size of an inductor's core strongly influence inductance. In traditional manufacturing of inductors, the area of the core can be manufactured with tight machine or model tolerance, and the permeability is a material property easily measured from the core material. For additive manufacturing processes, these characteristics are more challenging to control. The scope of printable metals is limited by the enhanced reactivity of nanoscale particles, and additive manufacturing approaches offer poorer reliability and control for fabricating with precise dimensional tolerance compared to more established methods. Moreover, disparate post-processing and curing requirements for different inks can lead to stresses and fracturing at interfaces of multi-material parts. This research focuses on addressing these challenges for additive manufacturing of miniaturized inductors.

### Design

To build a toroidal inductor using an additive manufacturing process, a multi-layer print was designed with two conductive layers of silver ink separated by a core of dielectric material. The first layer contains separate conductive triangular sections arranged in a circle using silver ink, following the simulated toolpath shown in Figure 1a. The second layer printed with polyimide precursor ink acts as the core of the inductor, separating the conductive top and bottom layers, using the simulated toolpath shown in Figure 1b. Finally, the third layer, like the first layer, is printed using silver ink connecting each section of the bottom layer to the adjacent section in the bottom layer to complete the coil around the core of the inductor, with the simulated toolpath shown in Figure 1c.

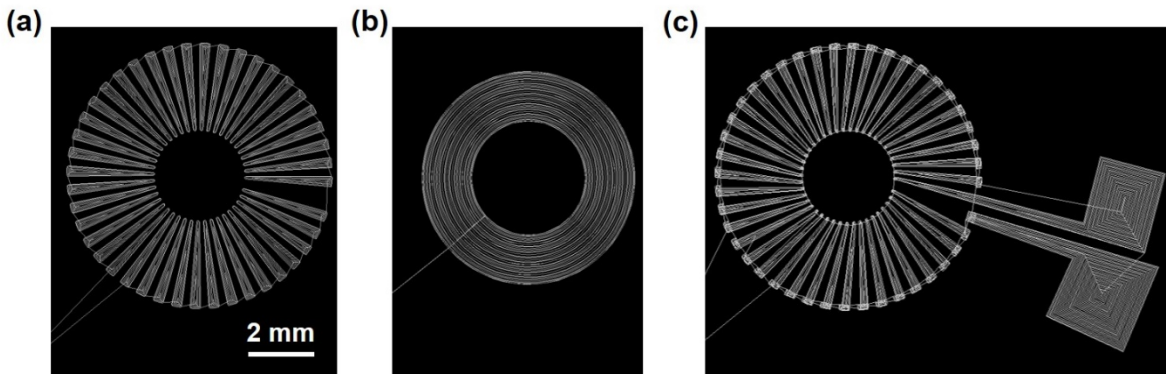


**Figure 1.** Toolpath simulations for printed layers 1-3 in (a)-(c), respectively.

### Motor Accuracy Limitations

Initial attempts to print layer 1 of the toroid revealed a problem with section sizes (individual triangles). Certain regions of the part exhibited larger sections than others, causing overlapping of sections in those regions and incomplete filling of those sections. Figure 2a displays this problem with the regions in the top left and bottom right having sections with much

larger area than adjacent sections. Having larger, unfilled, and overlapping sections would cause electrical shorting and poor conductivity in the inductor, lowering overall yield and performance.

To determine the cause of the print error in the larger regions, layer 1 was printed in three different ways. First, it was printed with no adjustments to provide a reference for comparison. Second, the X and Y axes were switched on the FlashCut control box to test the mechanics of the printer. Third, after putting the X and Y axes back to their original position on the control box, the toolpath was rotated 90 degrees to test the software of the printer. In all three prints no differences in defect occurrence was observed in the overall appearance of layer 1. Based on this, it was postulated that the precision of the X and Y motors was causing the problem. To test this hypothesis, layer 1 was printed at four times its initial size. When quadrupled in size, no sections with larger area were observed, fixing the overlap and infill issues and confirming the issue was due to the precision of the printer motors.

To achieve prints with the as-designed specifications, improvements in motor accuracy were required. The addition of gear reducers to both the X and Y axes motors with a 7:1 turning ratio, thus greatly improving the precision of the motors, sufficiently resolved the issue. After adding gear reducers, the sizing error was no longer observed, giving the required precision for the print. Figure 2b shows an image of layer 1 at normal size after adding gear reducers to the X and Y axes motors, demonstrating the effect of improved motor precision.

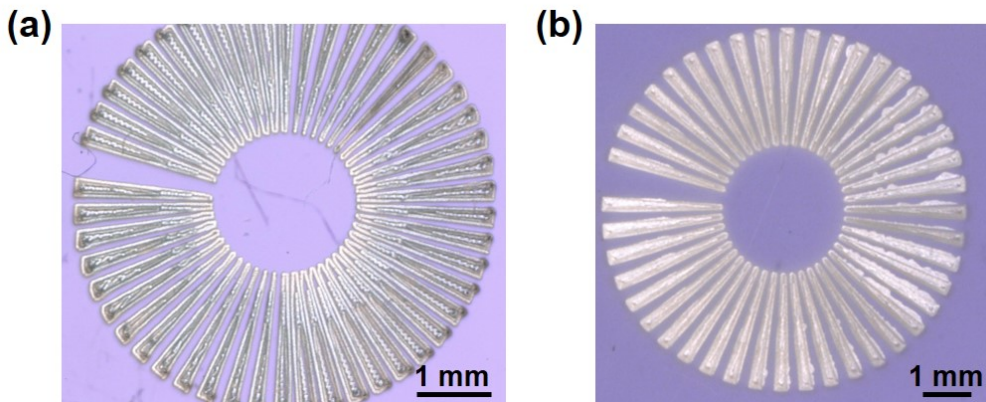


**Figure 2.** Layer 1 print before (a) and after (b) adding gear reducers to the X and Y motor axes.

#### Device Curing and Printing

To fabricate the inductor, each layer must be cured after printing, greatly increasing the overall manufacturing time. The bottom layer made of silver ink was printed first, followed by curing at 170 °C on a hot plate for 30 minutes. The second layer made from a polyimide precursor ink created the core of the inductor. This layer was cured in two steps to slowly evaporate solvents and prevent cracking, first at 80 °C for 60 minutes followed by 200 °C for 30 minutes. After curing layer 2, the final layer made of silver ink was printed to complete the coil. This layer was cured with the same parameters as layer 1 to complete the device. After curing of the polyimide, some cracking was observed in several inductors due to insufficient drying prior to the high temperature curing step. This issue will be solved as the manufacturing process is further optimized.

### **Measured vs. Designed Inductance**

After printing eight inductors, four devices successfully measured an inductance of  $\sim 1.5 \mu\text{H}$  at a frequency of 1 kHz, demonstrating the ability to successfully additively manufacture an inductor (Figure 3 shows microscope images of layers 1-3 during manufacturing). The four unsuccessful inductors failed due to a break in the coil, determined from an extremely high resistance that would be considered an open circuit. The four successful inductors exhibited a typical resistance of  $\sim 10 \Omega$ . To compare the measured inductance (additively manufactured) to an ideal part with the same dimensions, COMSOL was used to simulate the theoretical inductance. An optical microscope was used to measure the inner and outer diameter of the toroid, which were 2 mm and 6 mm, respectively, in line with the design. Stylus profilometry was used to measure the polyimide core height, shown in Figure 4, with a typical height of 15  $\mu\text{m}$  and deviations up to 55  $\mu\text{m}$  due to cracking of the polyimide film. Based on these values, COMSOL gave a theoretical inductance value of 0.07  $\mu\text{H}$ , much lower than measured. The cause for this disparity in measured and theoretical inductance is not fully understood at this point in the research. Future research will focus on accurate modeling and prediction for additively manufactured inductors based on design and printing parameters.

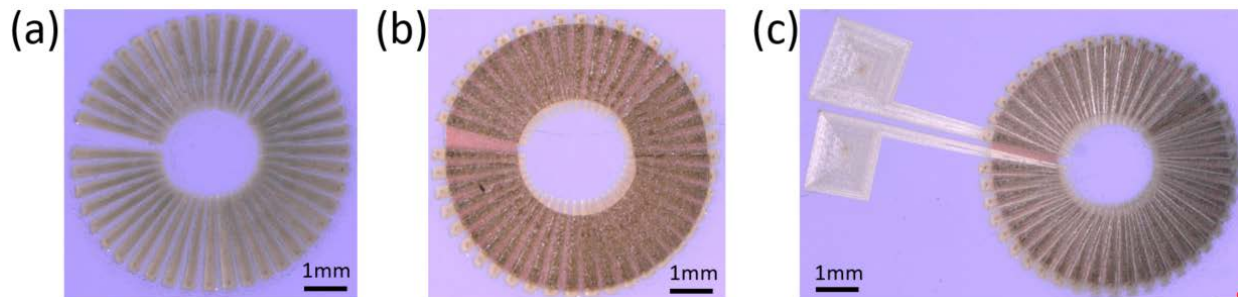


**Figure 3.** Inductor following printing of layers 1-3 in (a)-(c), respectively.

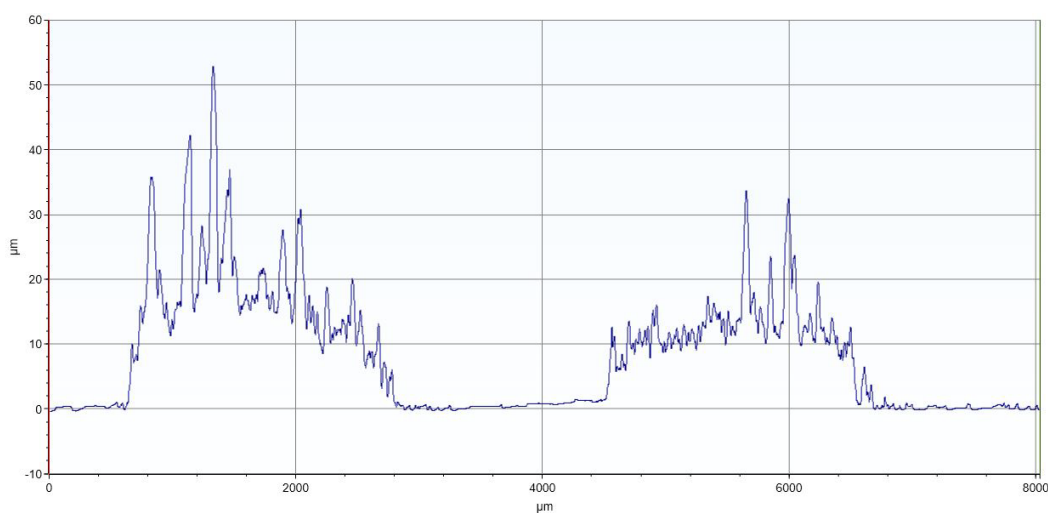


**Figure 4.** Profilometry measurement of additively manufactured inductor.

## **Future Work**

For future additive manufacturing of inductors, testing other designs, materials, and manufacturing techniques will be undertaken to more accurately predict inductance of a printed inductor and reach the final inductance requirement of 2  $\mu\text{H}$ . Toward this end, a new design for an inductor simulated to have 2  $\mu\text{H}$  inductance will be used for manufacturing. The permeability of the core will be increased by using a ferromagnetic material. Using a ferromagnetic core requires a 5-layer process that uses a dielectric (polyimide) to separate the conductive core from the conductive coil to prevent shorting of the inductor (layer 1: silver coil, layer 2: polyimide core, layer 3: ferromagnetic core, layer 4: polyimide core, layer 5: silver coil). In addition, a target core height of 50  $\mu\text{m}$  will increase the cross-sectional area to 0.156  $\text{mm}^2$ , and the number of turns in the coil will be increased from 43 to 50. Finally, increasing the outer diameter to 9.125 mm results in a circumference of 28.7 mm.

Future research and improvements for printed inductors include making the coil out of copper ink, to ensure improved compatibility with copper wire circuits, along with exploring the limits of core height to increase inductance. For printing copper, photonic sintering techniques will be considered, along with printing in an inert environment to prevent oxidization of metal nanoparticles. When increasing the core height with a rectangular cross section, the ability to connect the top and bottom of the coil due to the vertical sides of the core will get more and more difficult as the height increases. To prevent this issue, printing a core with a trapezoidal cross section will offer the ability to print on the slanted sides (trapezoidal) of the core instead of vertical sides (rectangular) of the core.

Overall, this work demonstrates a promising method for microinductor fabrication using a digital, direct-write additive printing method. Further research to improve manufacturing consistency and better correlate part design and print parameters with performance will further the multi-material fabrication of integrated systems, allowing smaller and more easily incorporated electronics components.

## **Acknowledgement**

Sandia National Laboratories is a multimission laboratory managed and operated by National Technology & Engineering Solutions of Sandia, LLC, a wholly owned subsidiary of Honeywell International Inc., for the U.S. Department of Energy's National Nuclear Security Administration under contract DE-NA0003525. This paper describes objective technical results and analysis. Any subjective views or opinions that might be expressed in the paper do not necessarily represent the views of the U.S. Department of Energy or the United States Government. This document has been released as Unclassified Unlimited Release, SAND-7056 C.

The authors would like to thank the following people for assistance and input to this work: Eric Langlois, Zach Beller, Derek Reinholtz, Chase Kayser, Matthew Roach, and Benjamin Spangler.

## **References**

- [1] Sarabol, P.; Cook, A.; Clem, P. G.; Keicher, D.; Hirschfeld, D.; Hall, A. C.; Bell, N. S., Additive Manufacturing of Hybrid Circuits. *Annual Review of Materials Research* **2016**, *46*, 41-62.
- [2] Essien, M. Apparatuses and Methods for Stable Aerosol Deposition Using an Aerodynamic Lens System. US Appl. 14/927380, 2016.
- [3] Christenson, K. K.; Paulsen, J. A.; Renn, M. J.; McDonald, K.; Bourassa, J., Digital Printing of Circuit Boards Using Aerosol Jet. In *International Conference on Digital Printing Technologies*, Society for Imaging Science and Technology: 2011; pp 433-436.
- [4] Goth, C.; Putzo, S.; Franke, J., Aerosol Jet Printing on Rapid Prototyping Materials for Fine Pitch Electronic Applications. In *IEEE ECTC*, IEEE: Lake Buena Vista, FL, 2011; pp 1211-1216.
- [5] Saleh, M. S.; Hu, C.; Panat, R., Three-Dimensional Microarchitected Materials and Devices Using Nanoparticle Assembly by Pointwise Spatial Printing. *Science Advances* **2017**, *3*, e1601986.
- [6] Kamby, P.; Knott, A.; Andersen, M. A. E. Printed Circuit Board Integrated Toroidal Radio Frequency Inductors, In *IECON 2012 – 38<sup>th</sup> Annual Conference on IEEE Industrial Electronics Society*, IEEE: 2012; pp 680-684.